

# Structural performance of spandrels in stone masonry buildings



**C. Amadio, N. Gattesco, A. Dudine, R. Franceschinis, G. Rinaldin**

*Department of Civil Engineering and Architecture, University of Trieste, Italy*

## **SUMMARY:**

Masonry spandrels affect in-plane seismic performance of masonry walls in existing unreinforced masonry buildings, as they guarantee an effective coupling between adjacent masonry piers. In this work some results achieved in experimental tests carried out to investigate the structural response of unreinforced masonry spandrels under cyclic loads are presented. Three full-scale spandrel specimens were considered: two made of masonry bricks and one made of sandstone. The effectiveness of two strengthening techniques was investigated: CFRP strips glued horizontally on the spandrel surface and a horizontal steel angle fixed to the spandrel through injected dowels. Based on the above experimental results, a schematization of the resisting mechanism was developed and an analytical model to assess the capacity of spandrels was carried out.

*Keywords: ancient buildings, masonry spandrel, experimental tests, numerical model.*

## **1. INTRODUCTION**

Ancient masonry buildings (AMB) constitute a significant portion of existing buildings around the world. Many of these structures have a historical and cultural value and are considered as architectural heritage. Such buildings are made with brick or stone masonry walls and wooden floors or masonry vaults that usually form the horizontal structural system. A large number of these buildings are located in seismic prone areas and have shown poor effectiveness under past earthquakes. An accurate structural assessment as well as the development of effective strengthening techniques is therefore of paramount importance for AMB. In fact, a rough analysis may lead to either overestimate or underestimate the safety of these structures. In the former case serious risks for human beings can be met, while in the latter case excessive strengthening measures, that cause high retrofitting costs and important changes in the original structures, could be requested. If the floor system in unreinforced masonry (URM) buildings is designed to distribute seismic actions to shear walls and to prevent out-of-plane displacements in the walls perpendicular to earthquake shakes, the seismic performance of URM buildings is governed mainly by the in-plane capacity of shear walls. In many cases they are perforated walls whose strength and stiffness are strongly influenced by the coupling between spandrels and piers. The first structural models for perforated walls under horizontal forces were based on simplified assumptions concerning the capacity of spandrels. In the strong pier-weak spandrel model, the strength of spandrels is neglected and only the piers, which span from the foundation to the roof of the building, withstand horizontal forces. Conversely, in the weak pier-strong spandrel model, the coupling masonry beams are assumed to be infinitely stiff and resistant, and the building collapse is associated only to a storey mechanism due to the shear collapse of the piers. Because of the strong assumption on the masonry spandrel behaviour, either model can fail to predict the actual capacity of perforated masonry shear walls.

In the last years a big effort has been devoted to defining effective analytical and numerical models tailored for AMB seismic assessment and for the strengthening design, as their seismic response dramatically differs from that of the modern structural systems (e.g. steel or concrete structures).

Several models according to different theoretical approaches have been developed so far. Many of such models are used for research and, being based on complex finite element formulations (Lourenço, 1996), are high computationally demanding, so that they cannot be employed for realistic analyses of whole buildings. Different models have been developed for this last purpose; most of them use one-dimensional macro-elements to model the masonry wall so the seismic performance of whole buildings can be assessed with an acceptable computational effort. Therefore, in last nineties, improved numerical models based on the equivalent frame approach have been defined (e.g. Magenes and Calvi, 1997). In these models, suggested by the current design codes of practice (e.g. EN 1998 - 2004), FEMA 356 (1996), different failure mechanisms (i.e. shear with diagonal cracking, shear with sliding and rocking) are provided for each macro-element (Magenes, 2000). Such numerical models have been developed on the basis of both theoretical and experimental results. But, while many experimental outcomes (shear-compression test, diagonal compression test, etc.) on numerous types of masonry, even under cyclic loads are available for piers, to date very little tests have been carried out to study the actual behaviour of spandrels (Gattesco et al. 2010, Beyer and Dazio 2012). These experimental achievements are of paramount importance because the spandrel structural response is considerably different from that of the piers. In fact, under seismic loads, the masonry beams are subjected to shear and bending with negligible axial force. Therefore there is a need of experimental outcomes on masonry spandrels so to determine their actual behaviour in terms of both resistance and deformability. To make up for the lack of experimental data, the authors carried out an experimental study applying cyclic shear action on unreinforced masonry spandrels up to reaching the failure. Then, the specimens were reinforced with two different techniques and tested again.

## **2. TEST SET-UP**

Four experimental tests were carried out on full scale spandrels. Actually two specimens, made one with bricks and the other with rubbles, were tested as they are (unreinforced) and then they were strengthened, the former by gluing CFRP (carbon fiber reinforced polymer) strips on both surfaces and the latter by fixing a steel angle at one side through injected dowels (Gattesco and Macorini 2009), and tested again. The spandrels were subjected to a loading condition that simulates the actual state of stress occurring in a wall with openings, subjected to horizontal forces.

### **2.1. Specimens**

The test specimens are formed by a spandrel connected to the mid-height of two piers at their ends so to form an H shape. The piers length is equal to the distance between the mid-height of two consecutive floors of a representative building (Fig. 2.1a). One pier was fixed at both ends whereas the other was subjected to vertical translation maintaining both ends horizontal (Fig. 2.1b). The spandrel made with bricks (MS3) has the dimensions illustrated in Fig. 2.2a with a thickness equal to 38 cm whereas the one made with stones (MS4) has the dimensions illustrated in Fig. 2.2b with a thickness equal to 40 cm. The former specimen has a flat arch (25 cm thick) and a wooden lintel (12 cm) set over the opening whereas the latter has a wooden lintel on all spandrel thickness. As stated above, once completed the unreinforced test, the spandrel of specimen MS3 was strengthened (MS3r) by gluing on both lateral surfaces at the top and at the bottom CFRP strips, as illustrated in Fig. 2.2a. While the spandrel of specimen MS4 was strengthened (MS4r) with the application on one side of a steel angle (100x200x10 mm) connected to the masonry with injected threaded bars (Fig. 2.2b). The angle simulates the presence of a perimetric element used to connect and stiffen the wooden floor to the masonry (Gattesco and Macorini 2009).

### **2.2. Test arrangement**

The specimens have been built in the Laboratory for Testing Materials and Structures of the University of Trieste, Italy, in the position where they were tested. After about 60 days of air curing, the specimens were prepared for testing. One pier (Fig. 2.1a) was fixed to the stiff concrete basement through six vertical Dywidag steel bars. During construction and curing, the right pier was early laid

on provisional supports. A stiff steel element was placed on top of the pier and was connected to the bottom of the pier through six vertical Dywidag steel bars. The steel element was linked to three electro-mechanic actuators adequately fixed to the stiff concrete floor. Two actuators were arranged at both sides of the wall with their axis belonging to a plane perpendicular to the wall and containing the symmetry axis of the specimen, whereas the third actuator was set at the right side of the specimen. Two couples of steel braces were positioned on both sides of the specimen so as to contrast out-of-plane displacements of the wall (Fig. 2.3). Adequate sliding devices were provided at brace-wall interface; a thin layer of PTFE was used to reduce possible friction.

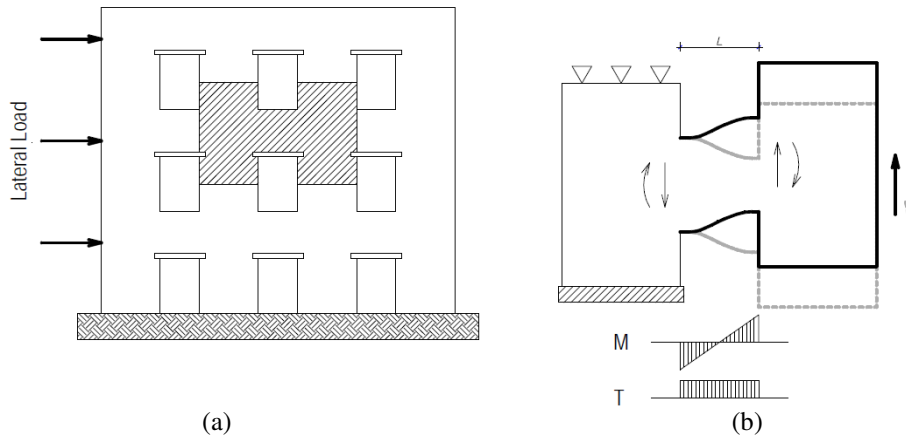


**Figure 2.1.** Masonry wall with openings (a); experimental model of the spandrel (b).

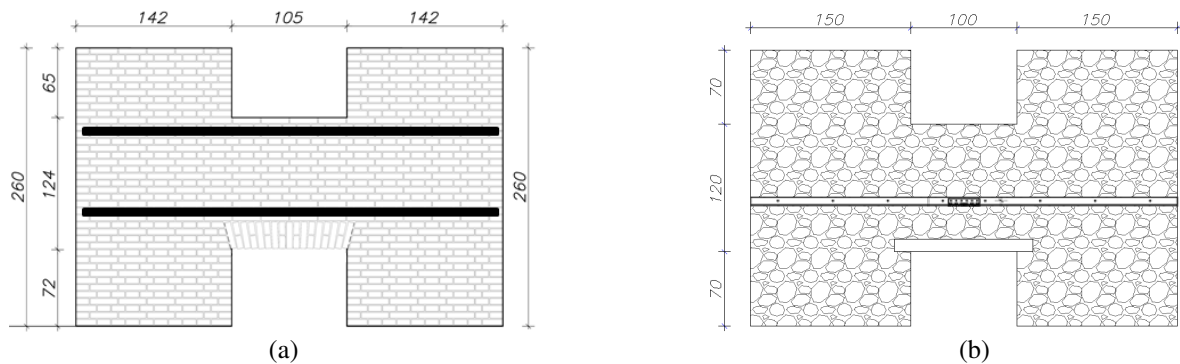


**Figure 2.2.** Brick specimen with CFRP strips (MS3r) (a); stone specimen with the steel angle (MS4r) (b).

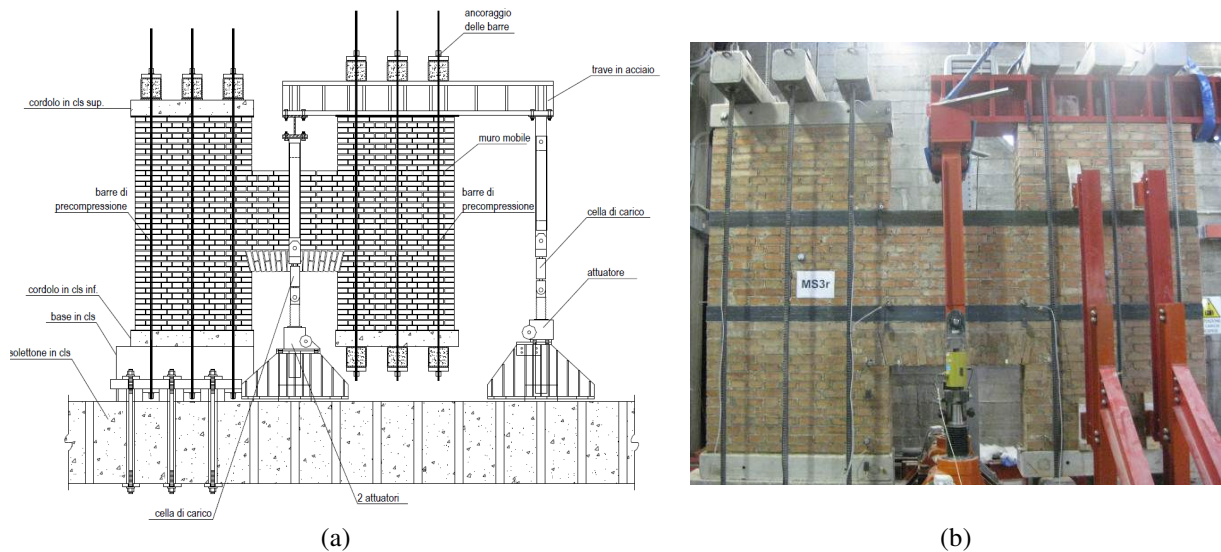


**Figure 2.3.** Experimental test arrangements: schematic drawing (a), axonometric view (b).

The steel bars were also used to apply a compressive force to the piers so as to simulate the axial load that normally acts in the wall due to gravity (self-weight, floor reaction, etc.). In particular, a distortion was applied to the bars in order to produce an average compressive stress equal to 0.5 MPa. Such a value corresponds to a common stress in a three-storey residential masonry building.

### **2.3. Loading system and gage location**

Many potentiometer LVDT (linear variable displacement transducers) were used to survey the displacements of several points of the specimens. In particular three transducers measured the vertical displacement of the steel element on the top of the right pier in correspondence of the point where the actuators were joined. Two couples of transducers were arranged to survey the vertical displacements of the bottom parts of the left and right piers, respectively. Two transducers measured the relative vertical displacements between the left and right mid points of the spandrel and the corresponding points at the bottom of the piers. Other two transducers were used for the horizontal displacements of two points at the ends of the spandrels, at top and bottom respectively. Two couples of instruments were used to measure the diagonal displacements on the spandrel's front and back side. Four inclinometers were also set to measure the rotation of some points of the specimen. Two inclinometers measured the rotation of the top of the left pier and the bottom of the right pier, respectively. Instead two inclinometers allowed to survey the rotation of both intersecting points among the piers and the spandrel axis. Three electro mechanic actuators (500 kN,  $\pm 150$  mm stroke) were used to apply the loads to the specimens while three loading cells, connected in series with the actuators, were used to survey the load. The electrical engines that moved the actuators were governed through a computer aided electronic unit.

### **2.4. Test procedure**

The actuators were forced to move together so to have the same vertical displacements. The tests were carried out by controlling the vertical displacements of the right pier forcing the stiff steel element on the top of the pier to remain horizontal during the test. The vertical displacement of all the actuators was varied cyclically between two opposite values that were gradually increased during the test. The test was endured in unreinforced specimens up to reaching a maximum vertical displacement equal to about  $\pm 8$  mm (1/125 of the spandrel length). In strengthened specimens the test was stopped when a significant damage in the spandrel occurred.

## **3. EXPERIMENTAL RESULTS**

The experimental results presented concern the tests carried out on the specimens described in Section 2.1. Some tests were carried out on samples of the mortar and the bricks used in the masonry wall specimens and on brick triplets so to determine some mechanical characteristics of the component materials of the specimen MS3. The average value of the compressive strength of the mortar was 2.12 MPa, the compressive strength of bricks was 44.81 MPa, the tensile strength of bricks was equal to 4.03 MPa and the shear strength at zero compressive stress for the masonry was equal to 0.14 MPa. The sample MS4 was made with rubbles; the mortar used have the same mechanical characteristics as that of specimen MS3.

The main results that summarize the global response of the spandrels in a masonry wall with openings concern the relationship between the shear load and the relative transversal end displacement of the spandrel. The shear load is the algebraic sum of the loads measured by the three loading cells arranged on the actuators. The displacement is obtained as the average of the transducers that measure the vertical displacement of the steel element on the top of the right pier. Such a value needs to be corrected in order to consider the rotation of the piers at the spandrel connection, which means on the basis of the rotations measured by the inclinometers. For each test, the whole sequence of loading and unloading is plotted in the following.

### 3.1. Samples MS3-MS3r

The relationship between the shear load and the relative transversal displacement of the unreinforced spandrel MS3 is shown in Fig. 3.1a. The test reached a maximum value of about 45 kN in both loading directions. After the peak load a quite rapid reduction in shear capacity was observed and a residual strength value of about 40-50% of the maximum shear was reached at the end of the tests in correspondence of a vertical displacement equal to 0.8% of the spandrel length. In Fig. 3.1b the crack pattern in the spandrel's back face at the end of the test is shown. As it can be seen the main cracks are diagonal (shear cracks).

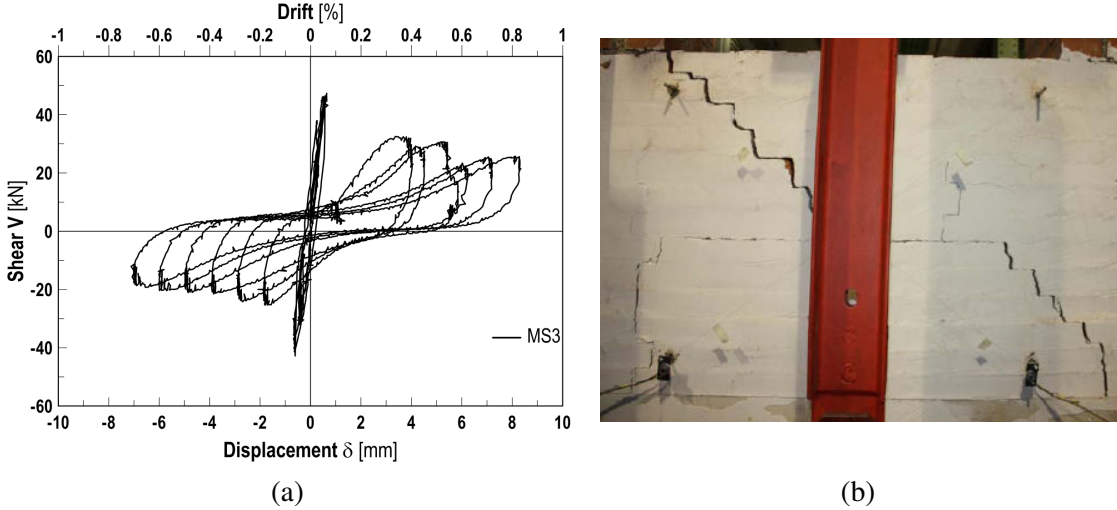


Figure 3.1. Specimen MS3: shear load against displacement (a) and crack pattern (b).

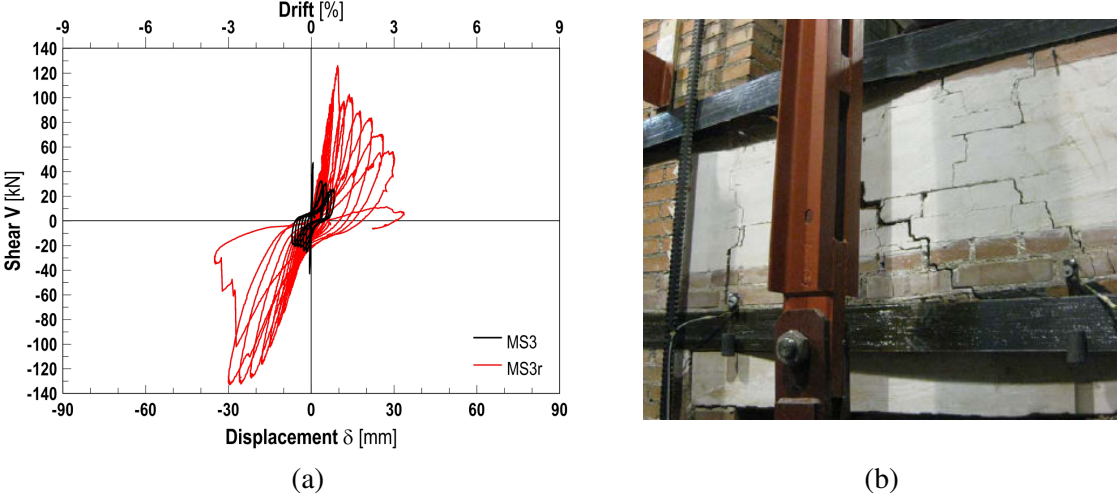


Figure 3.2. Specimen MS3r: shear load against displacement (a); crack pattern (b).

The sample MS3 was then reinforced (MS3r) applying horizontal CFRP strips. To close the cracks, after completing the unreinforced tests, a prestress was applied to the specimen using a couple of horizontal steel ties. By means of the steel ties (two Dywidag bars 27 mm diameter) a horizontal compressive force equal to 85 kN was applied to the spandrel. Two couples of horizontal CFRP strips (four CFRP strips, 120x1 mm) were glued on both sides of the spandrel. When the installation of the reinforcement was completed, the steel bars were released. The response in terms of shear load versus the relative vertical displacement of the reinforced specimen is shown in Fig. 3.2a (red line), the black curve is that obtained in unreinforced tests (Fig. 3.1a). A maximum resistance value of about 130 kN was reached (almost three times the resistance achieved with the unreinforced specimen). After the peak load a progressive reduction in shear capacity was observed, especially in one direction. In the other direction, a rapid decrease of resistance was observed, due to the local debonding on CFRP strips. The maximum drift is about 3%, so the increase in ductility was significant with respect to the

unreinforced spandrel (MS3). The same diagonal cracks occurred in unreinforced specimen reopened, as visible in Figure 3.2b, which refers to a loading step just before the collapse of the spandrel.

### 3.2. Samples MS4-MS4r

The shear load versus the relative vertical displacement of the unreinforced specimen MS4 is illustrated in Fig. 3.3a. The MS4 test reached a maximum value of about 28 kN in one direction and 20 kN in the opposite one. After the peak, the resistance was maintained constant up to a value of the vertical displacement equal to about 0.8% of the spandrel length, when the test was terminated. In Figure 3.3b the crack pattern in the spandrel’s back face at the end of the test is shown. As it can be seen the main cracks are vertical and are placed at the ends of the spandrel (flexural cracks).

As the sample MS3, at the end of test MS4 the cracks of the specimen were closed through a couple of steel bars. A steel angle (100x200x10 mm) was connected to the internal face of the wall at the level of the floor by means of dowels ( $\Phi=16$  mm) driven into the wall with a spacing  $i=50$  cm and injected with cement grout. The relationship between the shear load and the relative vertical displacement of the reinforced spandrel is shown in Fig. 3.4a (red line), the black curve is that of the unreinforced specimen (Fig. 3.3a) and it is reported for a direct comparison. A maximum resistance value of about 60 kN was reached, which is more than twice the resistance achieved with the unreinforced specimen. After the peak load, the resistance is maintained constant up to a drift of 0.5%, and then it decreases slowly. The test was terminated when the vertical displacement was about 8% of the spandrel length. At the end of the test, a significant damage was noted, nevertheless the residual resistance was from 60% to 85%. Diagonal cracks formed and the existing vertical cracks started to open again only when large values of the vertical drift were reached (Fig. 3.4b).

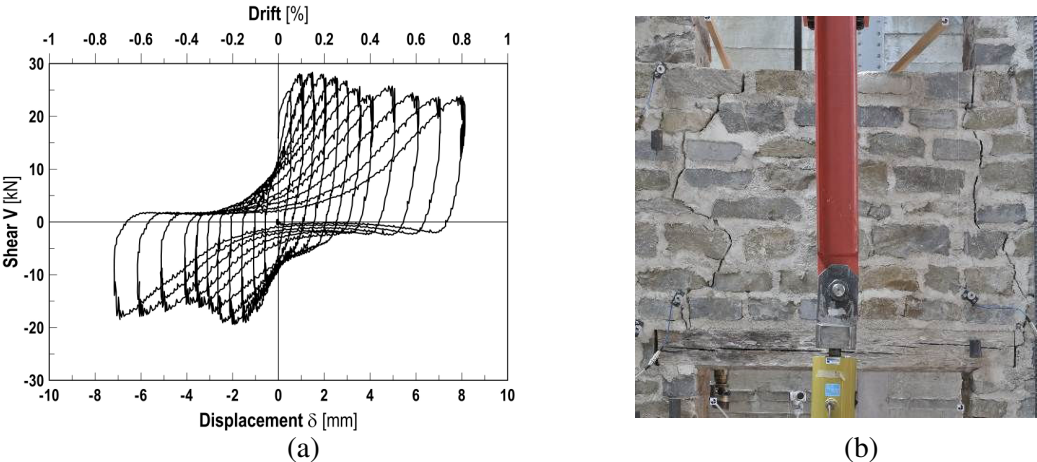


Figure 3.3. Specimen MS4: shear load against displacement (a) and crack pattern (b).

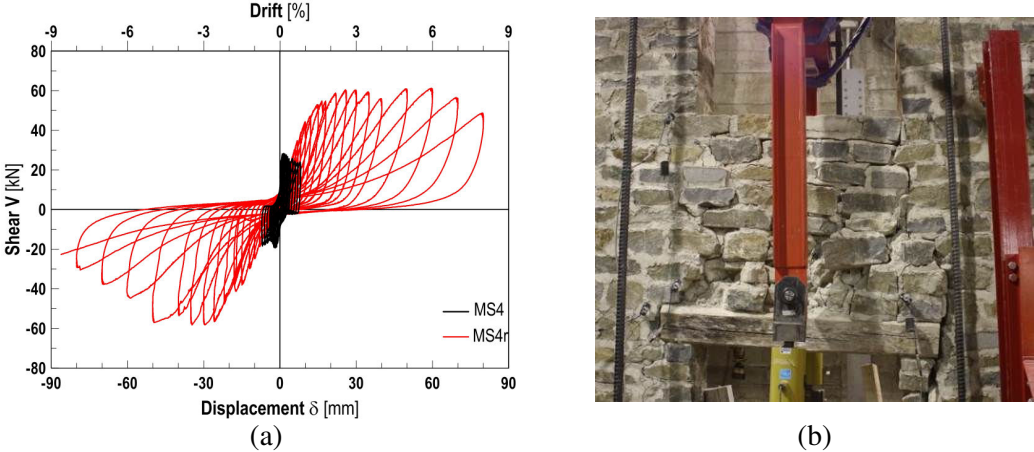
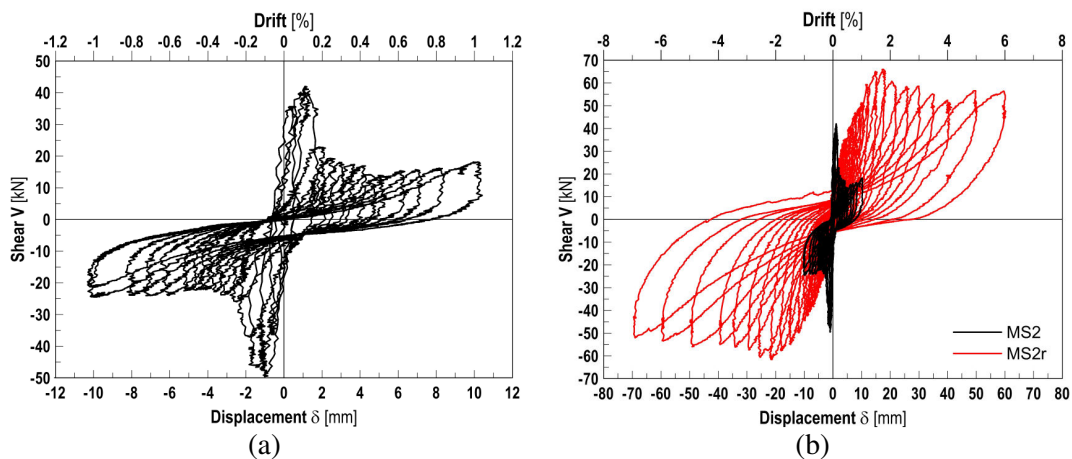


Figure 3.4. Specimen MS4r: shear load against displacement (a); crack pattern (b).

### 3.3. Considerations on the experimental results

To make some considerations on the experimental results obtained, a comparison with the results of the specimen MS2 reported in Gattesco et al. 2010, concerning a sample made with bricks, similar to specimen MS3, and strengthened through a horizontal steel angle fixed to the spandrel with injected dowels, as specimen MS4r was done. The results of specimen MS2 allow to evidence the effectiveness of the technique with steel angle on different masonry materials and to compare both the strengthening techniques studied applied to the same material of the masonry.

In Fig. 3.5a the shear load versus the relative transversal displacement of the unreinforced specimen MS2 is plotted. The curve shows a very similar behavior to that of specimen MS3 (Fig. 3.1a). As stated, specimen MS2r was strengthened using a steel angle fixed with dowels to the spandrel; the shear load against the relative vertical displacement is plotted in Fig. 3.5b. In the figure it is also reported in black the curve of the unreinforced specimen. It is evident an increase in the maximum shear with respect to unreinforced sample ranging from 150% to 200%. The shear resistance reduces very slowly after the peak up to values of the displacement equal to 7% the length of the spandrel.



**Figure 3.5.** Shear load against displacement: specimen MS2 (a); specimens MS2-MS2r (b).

The comparison of the results obtained with the two different strengthening techniques applied on brick masonry spandrels (MS2r-MS3r) evidences that a significantly greater increase in shear resistance may be obtained using the CFRP strips to strengthen the spandrel. In fact, in this case the shear resistance was almost tripled, whereas in the case of spandrel strengthened with the steel angle the shear resistance increase was from 50% to 100%. On the contrary, in the first case after the maximum value the shear resistance reduces quite rapidly and goes to collapse for a value of the vertical displacement not greater than 3%, whereas in the case of spandrel reinforced with the steel angle the shear resistance reduced very slowly and maintained a value greater than 60-85% up to vertical displacements equal to 8% the spandrel length. The cases analyzed evidence then a very different dissipative capacity. In the former case the different rapid resistance decrement is due to the brittle mechanism activated with the debonding of the CFRP strips (Fig. 3.2b). On the contrary, in the latter case the shear-displacement behavior is almost elastic-perfectly plastic.

Furthermore, the comparison of the results achieved with the same type of strengthening technique on different type of masonry specimens (samples MS2r, MS4r) evidences a similar behavior (Fig. 3.2a, Fig. 3.5b). The shear resistance increases to 150-200% that of the unreinforced specimen and the dissipative capacity is very high. In fact, in both cases a drift equal to 7-8% is reached conserving a very high residual shear resistance.

## 4. NUMERICAL MODELLING

With the aim to represent the spandrel behavior in an equivalent frame model, a numerical model has

been developed to represent and fit the results achieved for the spandrels tested. This model has been implemented in ABAQUS (Simulia 2010), a widely spread general finite element software, using its possibility to add to the solver custom finite elements. A user spring working in the plane of the wall has been developed, and some calibrations have been carried out and were presented afterwards (Amadio et al. 2011). The shear spring has been developed with non-linear cyclic capabilities; in the cases analysed the collapse is always due to shear strength. The model uses rigid beams and an elastic-plastic spring in the middle which simulates the shear behavior (Figure 4.1).

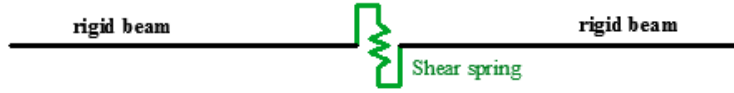


**Figure 4.1.** Model proposed for the spandrel behavior

This element represents the pure shear behavior of masonry spandrels, as the test results presented above, in which the hysteresis loops dissipate a great amount of energy per cycle. The assumed shape of hysteresis loop is that proposed by Tomazevic (1996). The envelope curve is tri-linear and origin-symmetric; it comprehends a linear elastic branch followed by a plastic branch with hardening and a third softening one. Hysteresis cycles are those from Tomazevic proposal (1996), which are composed by a first unloading branch with a degrading stiffness, followed by a pinching branch that ends to a point symmetrical to that at the beginning of the unloading.

The stiffness degradation is linear between elastic stiffness and ultimate stiffness and occurs in branches 4, 5, 40 and 50. The ultimate stiffness is chosen as input parameter by the user; in this work 80% of the elastic one was used. The strength degradation is implemented through an additional displacement that takes place in hysteretic cycles after peak resistance is reached ( $\Delta U$  in Fig. 4.2a). This displacement is directly proportional to the energy of an entire cycle through the parameter  $\beta$ , which was taken, as suggested by Tomazevic, equal to 0.06. Finally, the curve is characterized by an elastic stiffness calculated for a beam with ends restrained to rotation, by the shear strength calculated as explained afterwards, by inelastic stiffnesses (hardening and softening) equal to 1/10 of the elastic one, and finally by the peak resistance taken 30% greater than the elastic limit force. These parameters were taken from analyses carried out for masonry piers in (Amadio et al. 2011) and they have shown to be valid for spandrels too.

The shear strength is evaluated on the base of the following relations:

$$V_{Rd,F} = b \cdot t \cdot f_{vk0} \quad (4.1)$$

where  $b$  is the spandrel width,  $t$  is the thickness and  $f_{vk0}$  is the cohesive part of the shear strength. The strength to be assigned to the element is always the minimum value between the shear strength and that due to the bending resistance:

$$V_{Rd} = \min\left(\frac{2M_u}{L}; V_{Rd,F}\right) \quad (4.2)$$

where  $M_u$  is the ultimate flexural strength of the spandrel, calculated according to NTC (2008) and  $L$  is the spandrel length. A calibration has been made for MS3 and MS3r tests. In these cases, the spandrel has always a flexural strength greater than the shear mechanism one. For MS3 without reinforcements, the results are presented in Figure 4.3a. Also the test MS3r has been simulated numerically with the same routine. The shear strength associated to this test is calculated as the sum of two different terms; the former is the pure shear resistance, the latter is based on the mechanism that takes place in the masonry strip. The resultant shear strength has been evaluated as follows:

$$V_{Rd,tot} = V_{Rd} + V_{st} \quad (4.3)$$

where  $V_{Rd}$  pure shear strength, evaluated with Eqn. 4.2 in the case of undamaged spandrel, or shear residual strength if the spandrel is damaged. The relationship proposed in Eqn. 4.3 is always valid; only  $V_{st}$  can change its meaning accordingly to resisting mechanism. In this case the strut-tie mechanism caused by the presence of the CFRP reinforcements has to be considered. Referring to the Fig. 4.3b, CFRP strips increase the flexural strength of the spandrel (the strip in tension prevents from rocking) and give a shear contribution due to the vertical projection of the compressive strength of the diagonal strut ( $V_{st}$ ) formed in the masonry.

$$V_{st} = T_{lim} \tan(\beta) \quad (4.4)$$

$$T_{lim} = b_f \sqrt{2E_f t_f \Gamma_F} \quad (4.5)$$

where  $T_{lim}$  is the CFRP debonding strength,  $b_f$  is the width of CFRP strip;  $t_f$  is the thickness of CFRP strip;  $E_f$  is the Young modulus of CFRP strip in normal direction;  $\Gamma_F$  is the value of the specific fracture energy, evaluated according to CNR-DT 200 (2004). In any case, the strut compressive strength  $P$  cannot be greater than the masonry compressive strength. The dotted line in Fig. 4.3a,b was obtained numerically adopting Tomazevic's model. The results obtained are very close to the experimental curves and efficiently represents the spandrel shear behavior.

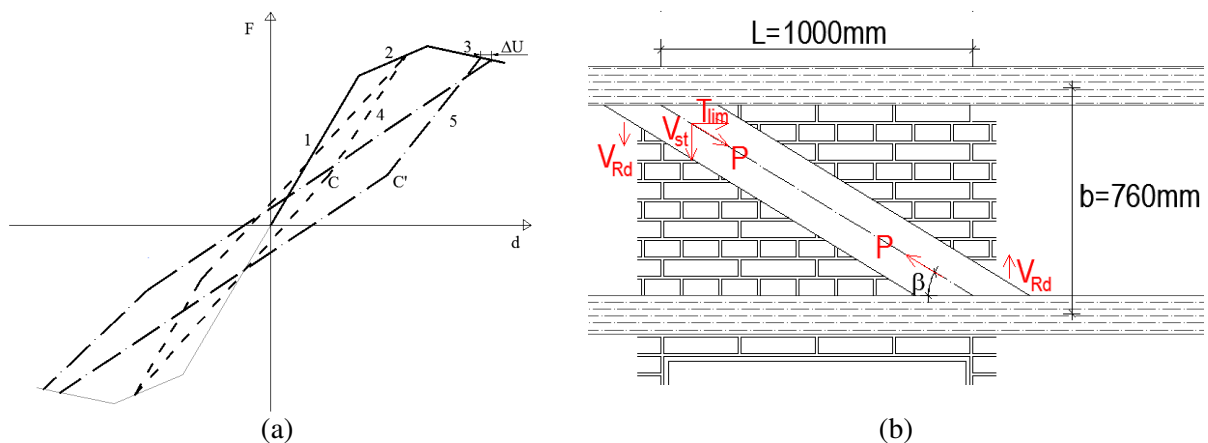


**Figure 4.2.** Hysteretic rules proposed by Tomazevic; dashed line evidences the typical cycle from first inelastic branch and dash-dot line represents the cycle from the second one (a) - Strut-tie mechanism in reinforced masonry spandrels (b)

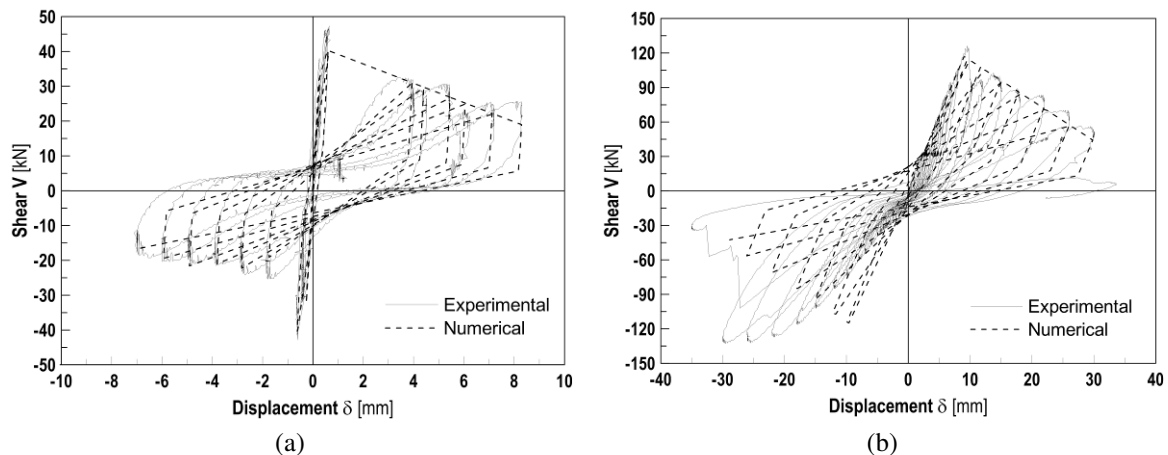


**Figure 4.3.** Experimental/numerical comparison on MS3 test (a) and MS3R (b)

## 5. CONCLUDING REMARKS

Two full scale samples of masonry spandrels, one made with bricks and the other made with rubbles, were subjected to shear test so to simulate the stresses due to the in-plane seismic excitation of the wall. At the end of the test they were strengthened, the former gluing CFRP strips on both surfaces and the latter fixing a steel angle at one side with injected dowels, and subjected to shear test again. The experimental results allow drawing some interesting remarks.

Unreinforced spandrels evidence a quite different response: the brick sample showed an almost elastic-brittle behavior with a residual resistance equal to 40-50% of the maximum shear capacity whereas the stone spandrel showed a behavior elastic-perfectly plastic up to significant values of the vertical displacement (0.8% of the spandrel length). The results concerning the strengthened samples evidence that the maximum shear resistance is almost tripled, in the first case (CFRP strips), and almost doubled in the second case (steel angle). After the peak value of the shear resistance a progressive reduction of the strength was observed in both samples. In the first case the reduction was quite fast due to the debonding of the CFRP strips and a residual resistance equal to 30% the maximum one was reached in correspondence of a vertical displacement equal to 3% of the spandrel length. In the latter case the reduction was very low and the residual resistance in correspondence of a vertical displacement equal to 8% the spandrel length was from 60% to 85%. A significant dissipative capacity was mainly evidenced in the specimen reinforced with the steel angle. Considering some previous experimental results it was possible to compare the effectiveness of both strengthening techniques on brick masonry spandrels and to check the improvement features of the technique based on the application of the steel angle on different masonry types (brickworks and course rubbles). The effectiveness of the steel angle reinforcement is appreciably greater in terms of dissipative capacity. The same technique showed similar features on both types of masonry.

The numerical model developed for simulating the cyclic behavior of the spandrel was tested with the experimental results. The experimental-numerical comparison evidences a very good reliability. The research is still on-going and other different types of masonry walls will be studied in future tests.

## ACKNOWLEDGEMENTS

The financial support of Italian Department of Civil Protection Reluis 2 (2010-2012) is gratefully acknowledged.

## REFERENCES

- Amadio C., Rinaldin G., Macorini L. (2011) An equivalent frame model for nonlinear analysis of unreinforced masonry buildings under in-plane cyclic loading, *Proceedings*, ANIDIS2011 Bari.
- Beyer K., Dazio A. (2012), Quasi-static cyclic tests on masonry spandrels. Acc. for pub. in *Earthquake Spectra*.
- CNR-DT 200 (2004) Istruzioni per la progettazione, l'esecuzione e il controllo di interventi di consolidamento statico mediante l'utilizzo di compositi fibrorinforzati – in Italian.
- EN 1998 (2004) Eurocode 8: Design of Structures for Earthquake Resistance - Part 3: Assessment and retrofitting of buildings, CEN, Brussels, Belgium.
- FEMA 356 (1996) Prestandard and commentary for the seismic rehabilitation of buildings, Federal Emergency Management Agency, Washington DC, USA.
- Gattesco N., Macorini I., Novel engineering techniques to improve the in-plane stiffness of wooden floors, *Proc.Int. Conf. On protection of historical buildings*, PROITECH 09, Rome, Italy, 21-24 June.
- Gattesco N., Macorini I., Clemente I., Noè S., (2010) Shear resistance of spandrels in brick-masonry buildings, *Proc. 8<sup>th</sup> Int. Masonry Conference*, IMS, 4-7 July, Dresden, Germany.
- Lourenço, P. B. (1996) Computational strategy for masonry structures. *PhD Thesis*, Delft University of Technology, Delft, the Netherlands.
- Magenes, G., Calvi, G.M. (1997). In-plane seismic response of brick masonry walls. *Earthquake Engineering Struct. Dyn.* 26, pp. 1091-1112.
- Magenes, G. (2000) Method for pushover analysis in seismic assessment of masonry buildings, proceeding, *Twelfth World Conference on Earthquake Engineering*, Auckland, New Zealand.
- NTC 2008 (2008) - D.M. 14-01-2008 - Norme tecniche per le costruzioni, building code, in Italian.
- Simulia (2010) ABAQUS User's Manuals, version 6.9-1
- Tomazevic M., M. Lutman (1996) Seismic behavior of masonry walls - Modeling of hysteretic rules, *Journal of Structural Engineering*.